

# CD19 targeting of chronic lymphocytic leukemia with a novel Fc-domain–engineered monoclonal antibody

Farrukh T. Awan,<sup>1</sup> Rosa Lapalombella,<sup>1</sup> Rossana Trotta,<sup>2</sup> Jonathan P. Butchar,<sup>3</sup> Bo Yu,<sup>4</sup> Don M. Benson Jr,<sup>1</sup> Julie M. Roda,<sup>1</sup> Carolyn Cheney,<sup>1</sup> Xiaokui Mo,<sup>5</sup> Amy Lehman,<sup>5</sup> Jeffrey Jones,<sup>1</sup> Joseph Flynn,<sup>1</sup> David Jarjoura,<sup>5</sup> John R. Desjarlais,<sup>6</sup> Susheela Tridandapani,<sup>3</sup> Michael A. Caligiuri,<sup>1</sup> \*Natarajan Muthusamy,<sup>1</sup> and \*John C. Byrd<sup>1</sup>

<sup>1</sup>Division of Hematology-Oncology, Department of Medicine, College of Medicine, <sup>2</sup>Department of Molecular Virology, Immunology, and Medical Genetics, <sup>3</sup>Division of Pulmonary Medicine, Department of Medicine, College of Medicine, <sup>4</sup>Department of Chemical Engineering, and <sup>5</sup>Center for Biostatistics, The Ohio State University, Columbus; and <sup>6</sup>Xencor Inc, Monrovia, CA

**CD19 is a B cell–specific antigen expressed on chronic lymphocytic leukemia (CLL) cells but to date has not been effectively targeted with therapeutic monoclonal antibodies. XmaB5574 is a novel engineered anti-CD19 monoclonal antibody with a modified constant fragment (Fc)–domain designed to enhance binding of Fc $\gamma$ R1IIa. Herein, we demonstrate that XmaB5574 mediates potent antibody-dependent cellular cytotoxicity (ADCC), modest direct cytotoxicity, and antibody-dependent cellular phagocytosis but not complement-mediated cytotoxicity against CLL cells. Interestingly, XmaB5574 mediates significantly higher ADCC compared with both the humanized anti-CD19 nonengineered antibody it is derived from and also rituximab, a therapeutic antibody widely used in the treatment of CLL. The XmaB5574-dependent ADCC is mediated by natural killer (NK) cells through a granzyme B–dependent mechanism. The NK cell–mediated cytolytic and secretory function with XmaB5574 compared with the nonengineered antibody is associated with enhanced NK-cell activation, interferon production, extracellular signal-regulated kinase phosphorylation downstream of Fc $\gamma$  receptor, and no increased NK-cell apoptosis. Notably, enhanced NK cell–mediated ADCC with XmaB5574 was enhanced further by lenalidomide. These findings provide strong support for further clinical development of XmaB5574 as both a monotherapy and in combination with lenalidomide for the therapy of CLL and related CD19<sup>+</sup> B-cell malignancies. (Blood. 2010;115:1204-1213)**

**icity against CLL cells. Interestingly, XmaB5574 mediates significantly higher ADCC compared with both the humanized anti-CD19 nonengineered antibody it is derived from and also rituximab, a therapeutic antibody widely used in the treatment of CLL. The XmaB5574-dependent ADCC is mediated by natural killer (NK) cells through a granzyme B–dependent mechanism. The NK cell–mediated cytolytic and secretory function with XmaB5574 compared with the nonengineered antibody is associated with enhanced NK-cell activation, inter-**

**feron production, extracellular signal-regulated kinase phosphorylation downstream of Fc $\gamma$  receptor, and no increased NK-cell apoptosis. Notably, enhanced NK cell–mediated ADCC with XmaB5574 was enhanced further by lenalidomide. These findings provide strong support for further clinical development of XmaB5574 as both a monotherapy and in combination with lenalidomide for the therapy of CLL and related CD19<sup>+</sup> B-cell malignancies. (Blood. 2010;115:1204-1213)**

## Introduction

Immunotherapy using monoclonal antibodies (MAbs) is an effective and safe method for the treatment of lymphoid malignancies.<sup>1</sup> Rituximab is a chimeric anti-CD20 MAb that was approved for marketing in 1997 and is widely used for the therapy of B-cell lymphoma. Alemtuzumab is another antibody targeting CD52 that is approved for use in relapsed chronic lymphocytic leukemia (CLL) but is associated with significant toxicity because of the ubiquitous expression of the target antigens on most normal immune cells including T cells and natural killer (NK) cells. On the basis of the success and limitations of rituximab and alemtuzumab, identification of alternative antibodies targeting alternative antigens on B cells represent an exciting strategy to pursue in B-cell malignancies.

The CD19 antigen is one such potential antigen on the surface of both normal and transformed B cells but has not been explored as a potential therapeutic antibody target. CD19 is a 95-kDa glycoprotein member of the immunoglobulin (Ig) superfamily and is expressed on follicular dendritic cells and all B cells from their early pre-B cell stage until the time of plasma cell differentiation.<sup>2,3</sup> CD19 surface expression is tightly regulated during B-cell development with higher levels seen in more mature cells and CD5<sup>+</sup>(B-1) B cells.<sup>2,4</sup> CD19 is expressed on the surface of B cells as a multiple molecular complex with CD21, CD81, and CD225<sup>5</sup> and is involved

in cosignaling with the B-cell receptor.<sup>6</sup> CD19-deficient mice have been shown to have normal B-cell maturation<sup>7</sup> but decreased proliferative capacity and impaired humoral responses.<sup>7-9</sup> This suggests that the effects of a CD19 targeting agent may result in the depletion of both malignant, immature B cells from the lymph nodes and the bone marrow and mature B cells from the circulation.

To date, clinical studies examining CD19 therapeutic antibodies have been limited and directed at B-cell lymphoma.<sup>10</sup> Hooijberg et al<sup>11</sup> have demonstrated inferior tumor engraftment protection, growth inhibition, NK-cell antibody–dependent cellular cytotoxicity (ADCC), and monocyte ADCC with several anti-CD19 murine antibodies compared with anti-CD20 murine antibodies. Recent developments in novel antibody engineering technologies have allowed modification of antigen binding and effector domains of therapeutic antibodies that render efficient target killing and innate immune activation functions.<sup>12</sup> XmaB5574 is an IgG1, humanized MAb targeting the CD19 antigen that was developed by Xencor Inc with the use of innovative antibody engineering technology.<sup>12</sup> XmaB5574 contains a modified constant fragment (Fc)–domain with 2 amino acid substitutions S239D and I332E that enhances its cytotoxic potency by increased affinity for activatory Fc $\gamma$  receptor IIIa on effector cells and diminished binding to Fc $\gamma$ RIIb.<sup>13</sup> Herein, we explore the preclinical activity of the novel engineered antibody

Submitted June 22, 2009; accepted November 4, 2009. Prepublished online as *Blood* First Edition paper, December 2, 2009; DOI 10.1182/blood-2009-06-229039.

\*N.M. and J.C.B. contributed equally to this study and are equal senior authors on this paper.

The publication costs of this article were defrayed in part by page charge payment. Therefore, and solely to indicate this fact, this article is hereby marked “advertisement” in accordance with 18 USC section 1734.

© 2010 by The American Society of Hematology

XmAb5574 in CLL and demonstrate that, unlike earlier antibodies, it has preclinical features, suggesting it to be an excellent candidate for future clinical development in this disease.

## Methods

### Patient sample processing and cell culture

All patients enrolled in this study had immunophenotypically defined B-cell CLL as outlined by criteria from the National Cancer Institute Working Group in 1996.<sup>14</sup> Blood was obtained from patients after written informed consent in accordance with the Declaration of Helsinki under a protocol approved by the institutional review board of The Ohio State University. Enriched B-cell CLL fractions were negatively selected as previously described.<sup>15</sup> Isolated CLL cells were incubated in RPMI 1640 media supplemented with 10% heat-inactivated fetal bovine serum (Hyclone Laboratories), 2mM L-glutamine (Invitrogen), and penicillin/streptomycin (56 U/mL/56 µg/mL; Invitrogen) at 37°C in an atmosphere of 5% CO<sub>2</sub>. Freshly isolated CLL cells were used for all studies. Samples used were greater than 90% B cells as determined by CD19 surface staining and fluorescence-activated cell sorting (FACS) analysis. Human NK cells (> 75%-80% CD56<sup>+</sup>, < 1% CD3<sup>+</sup>) derived from patients with CLL or healthy donors were isolated directly from fresh whole blood by 30-minute incubation with NK-cell enrichment RS cocktail before Ficoll Hypaque density gradient centrifugation as described above for the B-cell CLL fractions.

### Reagents and antibodies

The modified XmAb5574 and XmAb5603 wild-type anti-CD19 antibodies were provided by Xencor Inc. XmAb5603 is an IgG1 analog of XmAb5574 with an identical variable fragment with a wild-type IgG1 Fc. Phycoerythrin (PE)-labeled mouse anti-human CD19 antibody, PE-labeled mouse anti-human CD56 antibody, fluorescein isothiocyanate (FITC)-labeled mouse anti-human CD107a antibody, PE- and FITC-labeled isotype control mouse IgG1, FITC-labeled annexin V, and propidium iodide (PI) were all purchased from BD Pharmingen. 7-AAD was obtained from Beckman Coulter. Rabbit anti-human phospho- (no. 9101) and total p44/42 mitogen-activated protein kinase (extracellular signal-regulated kinases 1 and 2 [Erk1/2]; no. 4695) antibodies for Western blotting were purchased from Cell Signaling Technology Inc. PD98059 was acquired from EMD Biosciences. Anti-GAPDH antibody (no. SC-47 724) was from Santa Cruz Biotechnology Inc. Alemtuzumab was produced by Genzyme Corporation and purchased commercially. Rituximab and trastuzumab were produced by Genentech and purchased commercially. Goat anti-human IgG antibody (Fcγ fragment-specific) was purchased from Jackson ImmunoResearch Laboratories. 3,4-Dichloroisocoumarin (DCI) and concanamycin A were purchased from Sigma-Aldrich. Lenalidomide was extracted, purified, and confirmed to be the pure active compound as described previously.<sup>15</sup>

### Preparation of Alexa Fluor 488-labeled antibodies for internalization studies

XmAb5574, XmAb5603, rituximab, and control IgG1-isotype antibodies were fluorescently conjugated by an amine-reactive compound, Alexa Fluor 488 5-SDP ester (Invitrogen). Antibody solution (1.0 mg/mL) was dialyzed with Slide-A-Lyzer Dialysis Unit against 0.1M sodium bicarbonate buffer solution for 2 hours. Alexa Fluor 488 5-SDP ester (1.2 µL) in DMSO solution of 10 mg/mL was added to the antibody solution in buffer (NaHCO<sub>3</sub>, pH 8.3) for 1 hour at room temperature. The resultant solution was placed into Slide-A-Lyzer dialysis tube and dialyzed against phosphate-buffered saline (PBS; pH 7.4) overnight. The resultant Alexa Fluor 488-conjugated antibodies were collected and diluted to specific concentration, sterilized with 200nM polymer membrane filter, and stored at 4°C. Freshly isolated patient CLL cells were incubated at a concentration of 1 × 10<sup>6</sup> cells/mL for different times with 1 µg of the respective antibodies at 37°C. Cells were washed once with cold acidic glycine buffer (50mM glycine, 150mM NaCl, pH 2.7) or twice with cold PBS.

FACS was used to analyze the mean fluorescence intensity (MFI) of Alexa Fluor 488-positive cells. Percentage of internalization was calculated for each antibody relative to the isotype (0% control) and no-acidic glycine wash (100% control) conditions by using the formula [MFI experimental – MFI isotype (0% control)]/[MFI 100% control – MFI isotype (0% control)] × 100, as described previously.<sup>16</sup>

### In vitro treatment of cells with antibodies

Cells were cultured in media at a density of 10<sup>6</sup> cells/mL immediately after isolation. All antibodies, including XmAb5574, XmAb5603, trastuzumab, and rituximab, were used at 10 µg/mL except for the dose-response studies. The cross-linker, goat anti-human IgG (anti-Fc) was added to the cell suspension 5 minutes after adding the primary antibodies, at a concentration 5 times that of the primary antibodies (ie, 50 µg/mL for 10 µg/mL). For all direct cytotoxicity experiments, a group of samples with the same concentration of trastuzumab treatment was applied as isotype control. In addition, a group of samples with no treatment was collected as media control, and a group treated with fludarabine (10µM) was also set up as a positive control for apoptosis.

### Laser scanning confocal microscopy

Binding and internalization of CD19 antibodies (XmAb5574 and XmAb5603) in B-CLL cells were examined by laser scanning confocal microscopy. B-CLL cells were incubated with anti-CD19–Alexa Fluor 488 for 1 hour or 4 hours at 37°C. The cells were then washed 3 times with PBS (pH 7.4), followed by fixation with 4% paraformaldehyde for 20 minutes at room temperature. Nuclei were stained with 20µM DRAQ5TM (Biostatus Limited) for 5 minutes at room temperature. The cells were cytospun on the glass slides, and the coverslips were mounted in Prolong Antifade (Invitrogen) for confocal microscopy observation. Fluorescence of anti-CD19 (green) and DRAQ5 (blue) were analyzed by using Zeiss 510 META Laser Scanning Confocal Imaging Systems and LSM Image software (Carl Zeiss MicroImaging Inc).

### Assessment of apoptosis by flow cytometry

The apoptosis of cells after incubation with antibodies was measured using annexin V/PI staining followed by FACS analysis. Cells cultured either in 12-well plates or culture flasks with indicated treatments were stained with 5 µL of annexin V–FITC and 5 µL of PI (10<sup>6</sup> cells in 200 µL of 1 × binding buffer; all BD Pharmingen), and kept in dark, at room temperature, for 15 minutes before resuspension with 400 µL of 1 × binding buffer and analyzed by flow cytometry. Unstained cell sample and cells stained with annexin V or PI only were also processed for compensation. Results were represented as follows: the percentage of total positive cells over media control = (percentage of annexin V- and/or PI-positive cells in the treated sample) – (percentage of total annexin V- and/or PI-positive cells in the media control). All flow cytometric analyses were performed with the use of a Beckman-Coulter FC500 flow cytometer. Ten thousand events were collected from each sample, and data were acquired in list mode and analyzed with the CPX software package (Beckman-Coulter).

### CDC and ADCC assays

For the complement-dependent cytotoxicity (CDC) assay, CLL cells (10<sup>6</sup>/mL) were suspended in RPMI 1640 media, media with 30% plasma from healthy donor blood sample, or media with 30% heat-inactivated (56°C, 30 minutes) plasma. Cells were then treated and analyzed as previously described.<sup>15</sup> Similarly, ADCC activity was determined as described previously<sup>15</sup> by standard 4-hour <sup>51</sup>Cr-release assay. <sup>51</sup>Cr-labeled target cells (5 × 10<sup>4</sup> CLL cells) were placed in 96-well plates after incubating them with 10 µg/mL of various antibodies for 30 minutes. Effector cells (NK cells from healthy donors or patients with CLL) were then added to the wells at indicated effector-to-target (E/T) ratios. Perforin, granzyme B, and Erk-pathway inhibitors were added to the NK-cell suspension 30 minutes before their incubation with target cells. After a 4-hour incubation, supernatants were removed and counted in a γ counter. The percentage of specific cell lysis was determined by the following formula: percentage of lysis = 100 × (ER – SR)/(MR – SR), where ER,

SR, and MR represent experimental, spontaneous, and maximum release, respectively. NK-cell viability after both the perforin/granzyme B and Erk1/2 inhibitor treatments was greater than 90% as assessed by annexin V/PI staining.

### Antibody-dependent cellular phagocytosis assays

Monocytes were isolated from healthy donor whole blood with the use of CD14<sup>+</sup> selection and verified to be at least 98% pure by using flow cytometry with PE-Cy7–conjugated anti-CD14. These were then plated onto 10-cm<sup>2</sup> dishes and treated with 20 ng/mL monocyte-colony stimulating factor (R&D Systems) every other day for 5 days to differentiate them into monocyte-derived macrophages (MDMs). Nonadherent cells were washed away with PBS, and the adherent macrophages were harvested and labeled with PKH-26 fluorescent membrane dye (Sigma-Aldrich). CLL cells were labeled with PKH-67 (Sigma-Aldrich) and incubated on ice for 1 hour with no antibody, trastuzumab, XmAb5603, XmAb5574, or rituximab (10 μg/mL each). MDMs and CLL cells were then cocultured at a 1:2 ratio for 2.5 hours at 37°C. Colocalization of the CLL dye with MDM dye was then measured with flow cytometry. The percentage of phagocytosing macrophages was counted as the percentage of macrophages positive for antibody-coated CLL cell dye – the percentage of macrophages positive for non-antibody-coated CLL cell dye.

### NK cell in vitro stimulation and supernatant assays

For in vitro NK-cell stimulation experiments, wells of a 96-well flat-bottom plate were coated with 20 μg/mL of respective antibody in PBS overnight at 4°C to immobilize the antibodies, washed with cold PBS, and then plated with freshly isolated NK cells at  $2 \times 10^5$  cells/well. CD107a-FITC or isotype control was added to the suspension at the start of the 4-hour incubation at 37°C. NK cells were harvested at the end of the 4-hour incubation period and stained with CD56-PE and analyzed by FACS for CD107a surface expression. For supernatant experiments, cell-free culture supernatants were harvested after 4 hours and analyzed for levels of interferon-γ (IFN-γ) by enzyme-linked immunosorbent assay (R&D Systems) as described previously.<sup>17</sup>

For signaling characterization and inhibition experiments, wells of a 6-well flat-bottom plate were coated with 10 to 20 μg/mL of respective antibody and then plated with freshly isolated NK cells at  $5 \times 10^6$  cells/well. NK cells were harvested after 10-minute incubation and immediately subjected to lysis and protein extraction. For Mek/Erk signaling cascade inhibition experiments, PD98059 was added to the NK-cell suspension 30 minutes before plating and stimulation by fixed antibody.<sup>18</sup>

### Western blotting

Whole NK-cell lysates were prepared and kept in –80°C as described elsewhere<sup>19</sup> with the addition of the protease and phosphatase inhibitors [2mM sodium orthovanadate, 0.004 μg/mL microcystin LR, 1mM phenyl methane sulfonyl fluoride, 1mM benzamide, and 1.04mM (4-2-aminoethyl) benzene sulfonyl fluoride, 15μM pepstatin A, 14μM E-64, 40μM bestatin, 20μM leupeptin, and 0.8μM aprotinin; all from Sigma]. Protein concentration in the lysates was quantified by the bicinchoninic acid method (Pierce). Lysates with 30 to 50 μg of total protein were loaded to each lane in sodium dodecyl sulfate–polyacrylamide gels (10% for phospho-Erk1/2) and transferred to 0.2-μm nitrocellulose membranes (Bio-Rad) after electrophoresis. Horseradish peroxidase–conjugated goat anti-rabbit IgG (no. 170-6515; Bio-Rad) for phospho-Erk1/2 and total Erk1/2 was used as secondary antibodies. Detection was performed with chemiluminescent substrate SuperSignal from Pierce.

### Statistical analysis

All statistical analyses were performed by biostatisticians in the Center for Biostatistics at The Ohio State University. Linear mixed models were used for modeling treatment effects, and patient or healthy donor random effects. Hypothesis testing used contrasts that directly answered primary questions, for example, interaction contrasts were used to directly test inhibitory or synergy hypotheses found in the experiments that test mechanism of action

and ADCC, respectively. Random effects associated with these contrasts were included or subsumed in the random effects portion of the models to avoid biased low estimates of the standard errors of the contrasts. Holm method was applied to adjust for multiplicity and to control the overall family wise type I error rate at  $\alpha = 0.05$ . Confidence intervals are provided to show the precision of the effect estimates. SAS software (Version 9.1; SAS Institute Inc) was used for all statistical analyses.

## Results

### XmAb5574 modestly internalizes in primary CLL cells

CD19-directed antibodies have previously been shown to internalize rapidly on binding to the target antigen in CD19<sup>+</sup> cell lines, which could confound therapeutic application of XmAb5574.<sup>20,21</sup> As part of our initial investigation we therefore sought to determine whether the engineered antibody, XmAb5574, internalizes after antigen binding to primary CLL cells. As shown in Figure 1A, after binding to primary CLL cells, XmAb5574 internalized more than did XmAb5603 or the anti-CD20 antibody rituximab (15.6% higher compared with XmAb5603; 95% CI, 9.0%-26.6%;  $P < .001$ ;  $n = 5$  and 22.1% higher compared with rituximab; 95% CI, 17.8%-35.5%;  $P < .001$ ;  $n = 5$ ). Examining higher concentrations of XmAb5574 or for an extended time period beyond 30 minutes as shown in Figure 1B shows that using a linear mixed model a linear trends in CD19 antibody internalization for the dose ( $P < .001$ ) and time ( $P < .001$ ) exposure is observed. Consideration of these findings relative to target concentrations of XmAb5574 targeted in clinical trials and also monitoring for antibody internalization as part of the phase 1 study will be important. Confocal microscopy analysis of uptake of Alexa Fluor 488–labeled CD19 antibodies (XmAb5574 and XmAb5603) for 1 hour or 4 hours confirmed that most of CD19 to be still expressed on the cell surface. (Figure 1C).

### XmAb5574 induces modest direct cytotoxicity and no CDC against primary CLL cells

Induction of apoptosis in B cells from patients with CLL has been well characterized with commonly used therapeutic antibodies such as rituximab,<sup>22,23</sup> alemtuzumab,<sup>23-25</sup> lumiliximab,<sup>26</sup> milatuzumab,<sup>27</sup> and human leukocyte antigen–DR antibodies.<sup>28</sup> To determine the effect of XmAb5574 on B-cell survival, CD19<sup>+</sup> cells from patients with CLL were treated with XmAb5574, XmAb5603, trastuzumab, and rituximab in the presence or absence of Fc-specific, goat anti-human IgG antibody (α-Fc) as a cross-linker for 24 and 48 hours. Given the potential of the Fc-specific crosslinking antibody to influence CD19 expression, we evaluated this and demonstrate no change in CLL cell expression of CD19 ( $P = .76$ ; data not shown). The cytotoxicity as detected by annexin V/PI staining is shown in Figure 1D. Both XmAb5603 and XmAb5574 mediated moderate cytotoxicity on crosslinking. No increase in apoptosis was observed with extended treatment to 48 hours (data not shown). The cytotoxicity of XmAb5574 in the presence of α-Fc was modestly higher compared with trastuzumab (7.4% increase; 95% CI, 2.0%-12.7%;  $P = .02$ ;  $n = 9$ ) and was not significantly different from rituximab (0.6% increase; 95% CI, –10.5% to 11.7%;  $P = .91$ ;  $n = 9$ ). XmAb5574 was not found to mediate cytotoxicity in a dose-dependent manner (cytotoxicity increased only 4.4% with doses ranging from 0.1 μg/mL to 25 μg/mL XmAb5574 at 24 hours;  $P$  for trend = .71 for trend; data not shown). Therefore, a dose of 10 μg/mL was selected for further

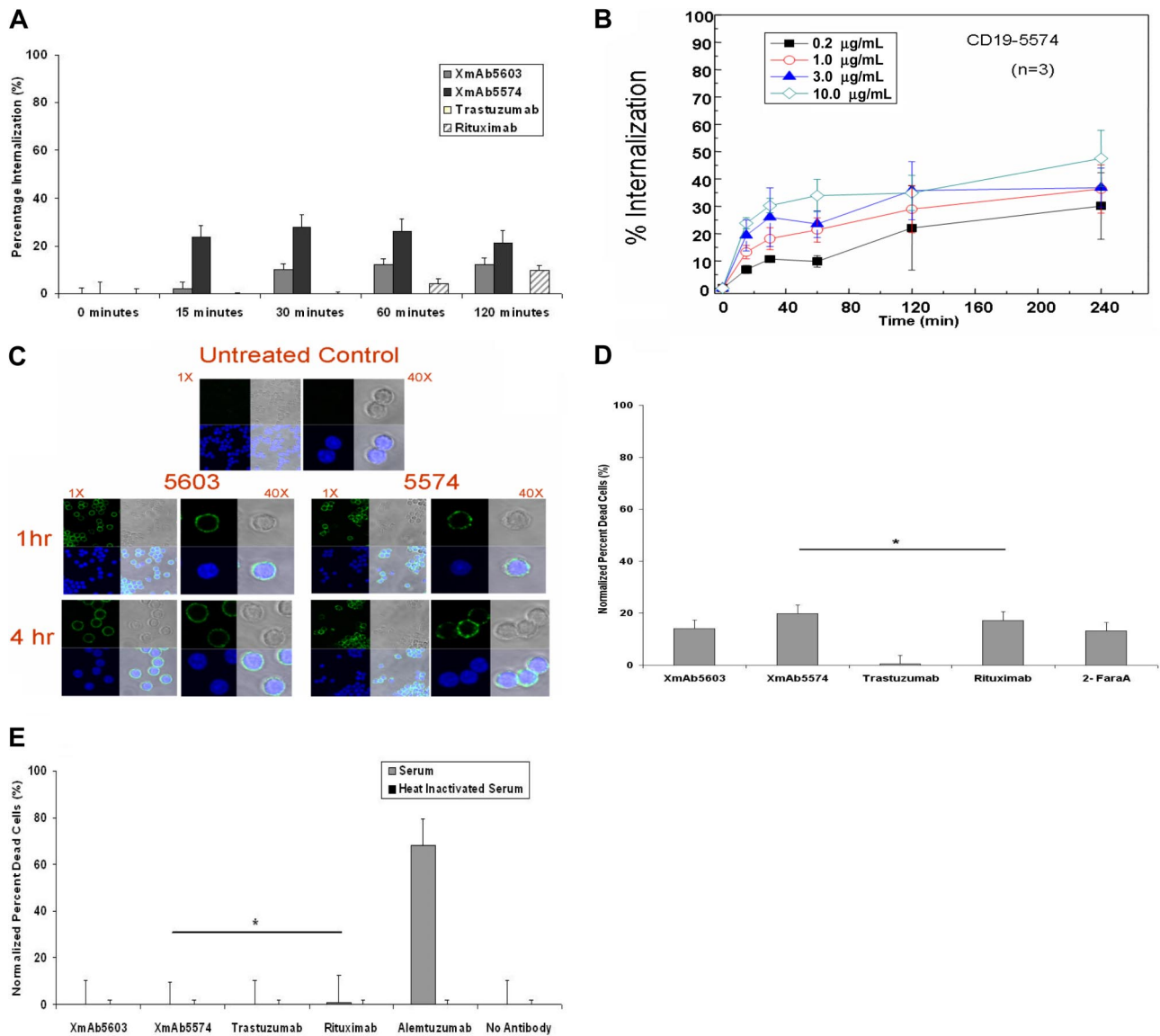


**Figure 1. Xmap5574 and Xmap5603 internalization studies and kinetics of CD19 antibody internalization.** (A) CLL cells from 5 patients were incubated with Alexa Fluor 488–labeled Xmap5574, Xmap5603, rituximab, and isotype control IgG1 antibodies, respectively, for indicated times and washed with either acidic glycine buffer to remove externally bound antibody or PBS. FACS was used to analyze the MFI of internalized antibody relative to the isotype (0% control) and no-acidic glycine wash (100% control) conditions by using the formula  $[(MFI_{\text{experimental}} - MFI_{\text{isotype (0\% control)}}) / (MFI_{\text{100\% control}} - MFI_{\text{isotype (0\% control)}})] \times 100$ . The average maximum internalization for Xmap5574 was 27.9% (95% CI, 14.5%–41.4%) at 30 minutes and for Xmap5603 12.2% (95% CI, 0.2%–24.3%) at 120 minutes of incubation. A plateau effect was also observed for antibody internalization at around 30 minutes of incubation ( $P$  for trend  $> .05$  for all antibodies tested). (B) Time and dose kinetics of CD19 antibody internalization. B-CLL cells were incubated with Alexa Fluor 488–labeled Xmap5574 (0.2, 1.0, 3.0, or 10  $\mu\text{g/mL}$ ) for indicated time periods. The cells were washed with either glycine buffer (100mM glycine, 50mM NaCl, pH 2.7) or PBS buffer (pH 7.4), and the percentage of internalization was determined as described in panel A. (C) Confocal microscopy analysis of uptake of fluorescently labeled CD19 antibodies in B-CLL cells in vitro. B-CLL cells were treated with Alexa Fluor 488 CD19 (Xmap5574 or Xmap5603) for 1 hour or 4 hours. After washing and fixation, the nucleus of cells were stained by DRAQ5. Images are shown in 1 $\times$  and 4 $\times$  magnifications. Fluorescence of anti-CD19 (green) and DRAQ5 (blue) were analyzed by using Zeiss 510 META Laser Scanning Confocal Imaging Systems and LSM Image software (Carl Zeiss MicroImaging Inc). (D) Xmap5574 induces minimal direct cytotoxicity in primary patient CLL cells. CLL cells from 9 patients were independently treated with media, goat anti-human IgG ( $\alpha\text{-Fc}$ ) and trastuzumab, Xmap5603, Xmap5574, or rituximab, all with and without  $\alpha\text{-Fc}$ , and 2-FaraA for 24 and 48 hours, and all at a concentration of 10  $\mu\text{g/mL}$ . Minimal cytotoxicity was observed at 24 or 48 hours (data not shown) after the addition of either Xmap5603 or Xmap5574. Even though Xmap5603 and Xmap5574 antibodies mediated direct cytotoxicity 6.2% (95% CI, 0.1%–11.6%;  $P = .02$ ) and 7.4% (95% CI, 2.0%–12.7%;  $P = .02$ ) more than trastuzumab, respectively, this difference may be of limited clinical utility. There was no difference in cytotoxicity mediated by Xmap5574 compared with rituximab in the presence of  $\alpha\text{-Fc}$  (0.6% increase with Xmap5574; 95% CI,  $-10.5\%$  to 11.7%;  $*P = .91$ ). The addition of  $\alpha\text{-Fc}$  to Xmap5574 also failed to significantly increase its direct cytotoxicity (0.4% increase; 95% CI,  $-8.9\%$  to 8.8%;  $P = .99$ ;  $n = 9$ ; data not shown). The direct cell death at 24-hour points for all cells was assessed by annexin V/PI staining and analyzed by FACS. Percentages of dead cells were calculated as the sum of annexin V $^{+}$  and/or PI $^{+}$  cells, and all values were normalized to media control. Error bars represent SEMs. (E) Xmap5574 does not induce CDC in primary CLL cells. CLL cells at 10 $^6$ /mL were treated with media, rituximab, trastuzumab, Xmap5603, Xmap5574, or alemtuzumab, all at a concentration of 10  $\mu\text{g/mL}$ , in the presence of media, media with 30% plasma from healthy donor blood sample, or media with 30% heat-inactivated (56 $^{\circ}\text{C}$ , 30 minutes) plasma for 1 hour. The CDC function was evaluated by PI staining on FACS analysis. Error bars represent SEMs. Xmap5574 does not mediate CDC against primary B-CLL cells (0.8% decrease; 95% CI,  $-4.5\%$  to 2.9%;  $P = .99$  compared with trastuzumab; and 2.9% decrease; 95% CI,  $-7.9\%$  to 2.1%;  $*P = .18$  compared with rituximab;  $n = 3$ ).

experiments on the basis of studies showing that other antibodies such as rituximab are saturated at 10  $\mu\text{g/mL}$  and also to provide equivalence of controls for the subsequently described effector cell studies that all used CLL cells as targets.

We next investigated whether the modified Fc-domain on Xmap5574 is efficient in mediating CDC against primary CD19 $^{+}$  CLL cells. Serum was obtained from healthy volunteers to perform CDC assays that showed the inability of Xmap5574 to mediate

CDC compared with rituximab ( $P = .36$  with Holm adjusted for 2 comparisons) or trastuzumab ( $P = .58$  unadjusted). Alemtuzumab as a relevant positive control resulted in significant CDC against primary CLL cells (Figure 1E).<sup>29</sup>

#### XmAb5574 mediates modest MDM-mediated antibody-dependent cellular phagocytosis against CLL cells

To evaluate the ability of XmAb5574 to enhance antibody-dependent phagocytosis of tumor cells, MDMs were incubated with CLL cells treated with no antibody, trastuzumab, XmAb5603, XmAb5574, or rituximab. The percentage of colocalization was not statistically different for XmAb5574 (12.37%; 95% CI, 7.78%-19.67%) compared with XmAb5603 (10.51%; 95% CI, 6.61%-16.7%;  $P = .58$ ;  $n = 6$ ) or rituximab (11.82%; 95% CI, 7.43%-18.79%;  $P = .87$ ; Figure 2A). All 3 antibodies showed significantly more MDM-mediated antibody-dependent cellular phagocytosis (ADCP) than did trastuzumab (adjusted  $P < .001$  for all). These results may be a reflection of the different isoforms of the Fc $\gamma$  receptors expressed on MDMs<sup>30,31</sup> and their role in mediating effector functions toward CD19-bearing tumor targets.

#### XmAb5574 enhanced NK cell-mediated ADCC against primary CLL cells

ADCC is efficiently mediated by binding and activation of NK cells through Fc-domain/Fc $\gamma$ RIIIa interactions. To determine

whether the Fc-engineered XmAb5574 induced efficient ADCC mediated by NK cells against patient CLL cells, we measured ADCC by the <sup>51</sup>Cr-release assay. Peripheral blood NK cells obtained from healthy volunteers mediated ADCC against allogeneic CLL cells in the presence of XmAb5574 but not in the presence of the negative control trastuzumab (Figure 2B). The difference between XmAb5574 and XmAb5603 at E/T ratio of 25:1 was 26.9% (95% CI, 14.5%-39.2%), which was significantly greater than the difference at E/T ratio 0:1 (difference was -3.0%; 95% CI, -15.4% to 9.3%). The  $P$  value for this synergistic interaction test was less than .001. For the comparison with rituximab at the highest E/T ratio used (25:1;  $n = 11$ ), XmAb5574 showed greater ADCC (33.5% higher; 95% CI, 20.8%-46.2%;  $P < .001$ ; Figure 2B).

More physiologically relevant, but technically difficult, is evaluation of antibody therapeutics with autologous-derived NK cells in conjunction with CLL tumor cells. We therefore studied the ability of XmAb5574 to induce ADCC by autologous NK cells against CLL cells. In this autologous setting lacking MHC mismatching seen with the use of allogeneic NK cells, we were able to demonstrate a similar, significantly higher magnitude of difference between cytotoxicity mediated by XmAb5574 compared with XmAb5603. The difference between XmAb5574 and XmAb5603 at E/T ratio of 25:1 was 23.6% (95% CI, 6.0%-41.2%), which was significantly greater than the difference at E/T ratio 0:1 (-7.9%; 95% CI, -25.5% to 9.7%). The  $P$  value for this synergy interaction test was .004. For the comparison with rituximab, we also found XmAb5574 to show greater ADCC (27.1% higher; 95% CI, 9.9%-44.3%;  $P = .002$ ;  $n = 5$ ) at E/T of 25:1 (Figure 2C). In addition, we confirmed a trend of increasing cytotoxicity mediated by

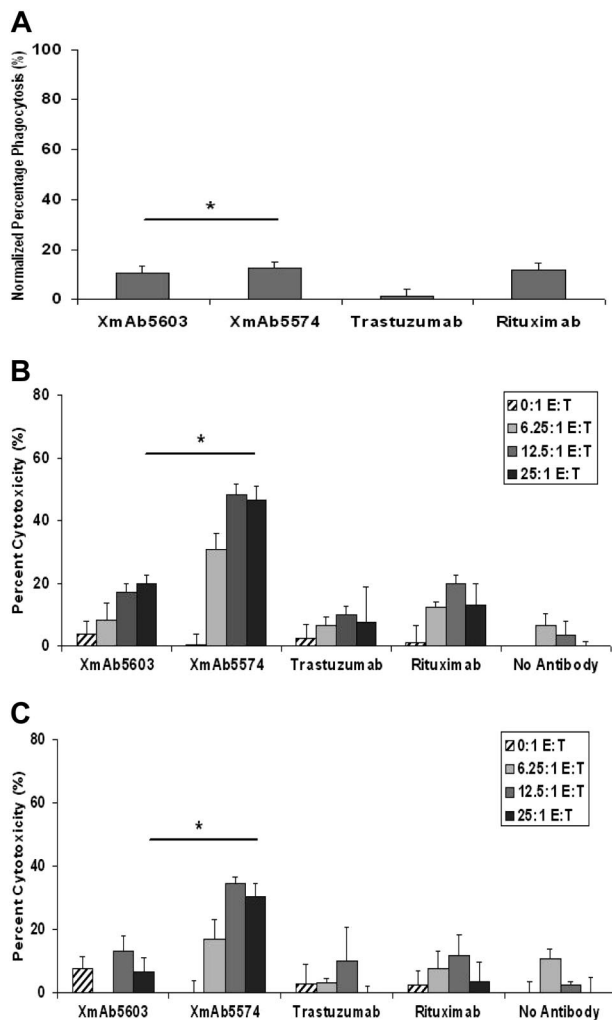


**Figure 2. XmAb5574 induces modest MDM-mediated ADCP against CLL cells.**

(A) CD14 selected monocytes isolated from healthy donor whole blood was used to derive macrophages under monocyte-colony stimulating factor and used in ADCP assays against primary patient CLL cells. Macrophages were harvested and labeled with PKH-26 membrane dye, whereas CLL cells were labeled with PKH-67 and incubated on ice for 1 hour with no antibody, trastuzumab, XmAb5603, or XmAb5574 (10  $\mu$ g/mL each). Macrophages and CLL cells were subsequently coincubated for 2.5 hours at 37°C and analyzed by FACS. XmAb5574 was unable to significantly enhance the MDM-induced ADCP against CLL cells compared with XmAb5603 (12.37% vs 10.51%; estimated ratio, 1.18; 95% CI, 0.61-2.27;  $P = .58$ ) or rituximab (11.82% phagocytosis; estimated ratio, 1.05; 95% CI, 0.54-2.02;  $P = .87$  compared with XmAb5574). XmAb5574 did, however, show a statistically significant increase in ADCP compared with our negative control trastuzumab (12.37% vs 1.18%; estimated ratio, 10.47; 95% CI, 5.43-20.17;  $P < .001$ ;  $n = 6$ ). An E/T ratio of 1:2 was used for all experiments. Percentage of phagocytosis was calculated as events positive for both PKH-67 and PKH-26 dyes. Error bars represent SEMs. (B-C) XmAb5574 induces potent ADCC by NK cells against both allogeneic and autologous B-CLL cells. XmAb5574 induced NK cell-mediated ADCC against allogeneic (B) and autologous (C) CLL cells. Ability of rituximab, trastuzumab, XmAb5603, or XmAb5574 to mediate ADCC was evaluated with the use of either fresh allogeneic or autologous human NK cells as effector cells and B-CLL cells as target cells at the indicated E/T ratios by standard 4-hour <sup>51</sup>Cr-release assay. <sup>51</sup>Cr-labeled target cells ( $5 \times 10^4$  CLL cells) were placed in 96-well plates after incubating them with 10  $\mu$ g/mL of various antibodies for 30 minutes and subsequently coincubating them with NK cells (from healthy donors or patients with CLL) at indicated ratios. Specific inhibitors were added to NK cells 30 minutes before cocubation. After 4-hour incubation, supernatants were removed and counted in a  $\gamma$  counter, and the percentage of specific cell lysis was determined by the following formula: percentage of lysis =  $100 \times (ER - SR) / (MR - SR)$ , where ER, SR, and MR represent experimental, spontaneous, and maximum release, respectively. (B) XmAb5574 induces progressively higher ADCC by allogeneic NK cells derived from healthy donors with increasing E/T ratios (24.1% increase; 95% CI, 12.9%-35.3%;  $P$  for trend  $< .001$ ) and significantly higher ADCC compared with XmAb5603 (26.9% increase; 95% CI, 14.5%-39.2%;  $P \leq .001$ , at the highest E/T ratio used of 25:1) or rituximab (33.5% increase; 95% CI, 20.8%-46.2%;  $P \leq .001$ ; at E/T of 25:1;  $n = 11$ ). (C) Similarly, with the use of autologous NK cells derived from the same patients with CLL there was a 23.9% progressive increase in ADCC with increasing E/T ratios (95% CI, 9.4%-38.3%;  $P = .006$ ). XmAb5574 was also able to significantly increase ADCC mediated by autologous NK cells compared with XmAb5603 (23.6% increase; 95% CI, 6.0%-41.2%;  $P = .01$ ; at E/T of 25:1) or rituximab (27.1% increase; 95% CI, 9.9%-44.3%;  $P = .0026$ ; at E/T of 25:1;  $n = 5$ ).

XmAb5574 with a higher E/T ratio (23.9% and 24.1% increase from E/T = 6.25 to 25:1; 95% CI, 9.4%-38.3% and 12.9%-35.3%;  $P = .006$  and  $P$  for trend  $< .001$ , in the autologous and allogeneic settings, respectively).

#### XmAb5574-mediated NK-cell ADCC against CLL cells is mediated predominantly by granzyme B

The mechanism by which NK cells mediate toxicity against XmAb5574-bearing CLL cells has not been explored previously. Direct and antibody-dependent NK-cell killing can occur by release of IFN- $\gamma$ , direct cell membrane perforation by perforin, or activation of caspases by granzyme B.<sup>32</sup> The incubation of NK cells with specific granzyme B inhibitor DCI before their coculture with target CLL cells resulted in a significant reduction in the magnitude of ADCC induced by XmAb5574 (18.0% decrease; 95% CI, 4.9%-31.2%;  $P = .008$ ;  $n = 29$ , compared with DMSO at E/T of 25:1; Figure 3A). The suppression of ADCC supports that granzyme B plays an important role in NK cell-mediated ADCC induced by XmAb5574. In contrast, perforin inhibitor at the tested concentration did not significantly alter XmAb5574 ADCC against CLL cells. Interestingly, the suppression of ADCC mediated by XmAb5603 was complete with granzyme B and perforin inhibitors unlike that observed with XmAb5574, suggesting the improved ability of XmAb5574 to overcome this inhibition at similar concentrations.

#### XmAb5574 functionally activates NK-cell CD107a production, IFN- $\gamma$ secretion, and Erk1/2 phosphorylation

XmAb5574 mediates improved ADCC through a granzyme B-dependent killing process. We next sought to confirm that this

enhanced ADCC by XmAb5574 was a consequence of enhanced NK-cell activation. Release of cytokines and cytolytic granzyme B that promotes NK-cell cytotoxicity occurs by a process of degranulation, during which time NK cells express lysosomal associated membrane protein-1 (CD107a) on their membrane which can be used as a surrogate for their cytotoxic potential.<sup>33</sup> We used resting NK cells from healthy donors and exposed them to fixed XmAb5574, XmAb5603, rituximab, or trastuzumab and evaluated the expression of CD107a on the surface of these NK cells to provide a functional assessment of the ability of XmAb5574 to activate NK cells. Fixed antibody conditions were used to perform these experiments, and after a 4-hour incubation period NK cells exposed to XmAb5574 had a much higher expression of CD107a compared with XmAb5603 (19.4% increase; 95% CI, 9.6%-29.2%;  $P = .005$ ;  $n = 5$ ), and compared with rituximab, the difference was 12.8% (95% CI, 0.2%-25.3%;  $P = .04$ ;  $n = 5$ ; Figure 4A). A representative density plot of enhanced CD107a induction by XmAb5574 in CD56<sup>+</sup> NK cells is shown in Figure 4B.

IFN- $\gamma$  release from NK cells is a critically important cytokine involved in innate immune-mediated tumor cell clearance and also activation of macrophages.<sup>34</sup> Production of IFN- $\gamma$  from NK cells can be stimulated by the engagement of Fc $\gamma$ R on the surface of NK cells and serves as a reliable marker of their activation.<sup>35,36</sup> To evaluate whether the differential ability of XmAb5574, XmAb5603, trastuzumab, and rituximab to activate NK cells is reflected in IFN- $\gamma$  secretion, we stimulated NK cells from healthy donors with plate-immobilized antibody for 4 hours. The supernatants were harvested and analyzed for the presence of soluble IFN- $\gamma$ . Consistent with the potent activation of NK cells as reflected by CD107a expression and ADCC function, Fc-modified XmAb5574 induced an approximate 6-fold increased production of IFN- $\gamma$  compared with the other nonengineered antibodies (XmAb5603, 6.4 times higher; 95% CI, 2.1-19.2;  $P = .007$ ;  $n = 4$ ; and rituximab, 5.95 times higher; 95% CI, 2.3-15.41;  $P = .004$ ;  $n = 4$ ) as shown in Figure 4C.

Erk1/2 of the mitogen-activated protein kinase family are serine-threonine kinases whose activation on phosphorylation is a prerequisite to Fc $\gamma$ RIIIa-induced granule exocytosis in NK cells.<sup>37-39</sup> To determine whether the increased NK-cell activation observed with XmAb5574 is reflected in Fc $\gamma$ RIIIa-induced downstream signal transduction mechanisms in NK cells, we used our immobilized antibody conditions described earlier to stimulate healthy donor NK cells and assessed Erk1/2 phosphorylation by immunoblot with the use of anti-phospho- and nonphospho-Erk1/2 antibodies. As shown in Figure 5A and B, compared with the control XmAb5603, XmAb5574 increased Erk1/2 phosphorylation that could be partially reversed by the addition of Erk1/2 inhibitor PD9809. A similar effect was observed in the reduction of ADCC in the presence of Erk1/2 inhibitor (Figure 5C). Collectively, these data provide distinct biochemical evidence of XmAb5574 antibody activation of NK cells compared with the parent antibody as measured by enhanced CD107a surface expression, IFN- $\gamma$  production, and Erk1/2 phosphorylation.

One preclinical concern that exists with Fc $\gamma$ R-engineered antibodies such as XmAb5574 is that enhanced ligation of the Fc $\gamma$ RIIIa on NK cells by either free or fixed antibody might promote intracellular signaling, leading to NK-cell death. Indeed, preclinical *in vivo* primate studies with XmAb5574 have shown transient depletion of circulating blood NK and B cells that could be a consequence of NK-cell death or such cells trafficking to antibody-bound tumor cells.<sup>40</sup> In Figure 5D we demonstrate that, despite enhanced activation of NK cells and enhanced Fc $\gamma$ RIIIa

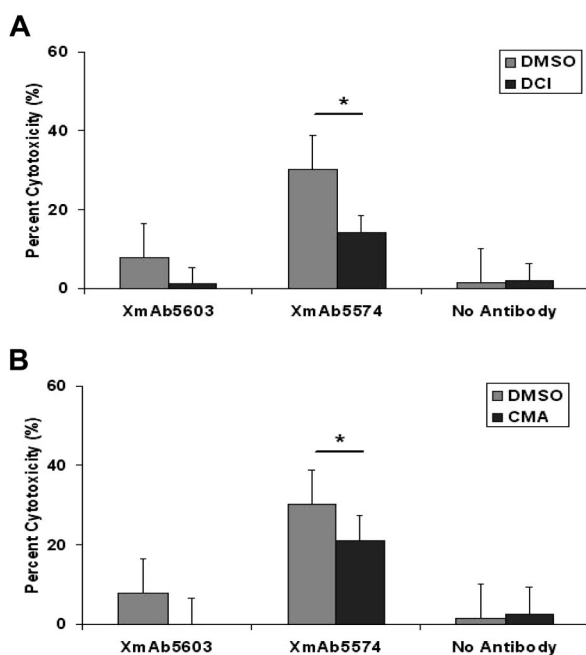


**Figure 3. XmAb5574-induced ADCC by NK cells against B-CLL cells is mediated through granzyme B and perforin-mediated pathways.** NK cells ( $10^6$  cells/mL) were treated with DMSO, granzyme B inhibitor DCI at  $10\mu\text{M}$  (A), or a perforin inhibitor concanamycin A (CMA) at  $50\text{nM}$  (B) for 30 minutes before incubation with allogeneic CLL cells. Ability of XmAb5574 to mediate ADCC against CLL cells through NK cells was diminished significantly in the presence of (A) DCI (17.4% decrease with DCI; 95% CI, 7.06-27.84;  $P = .007$ ;  $n = 29$ , compared with DMSO\* at E/T of 25:1) but not with (B) CMA (9.15% decrease with CMA; 95% CI, 1.2% to -19.49%;  $P = .23$ ;  $n = 29$ , compared with DMSO\* at E/T of 25:1) at the tested concentration. Error bars represent SEMs.

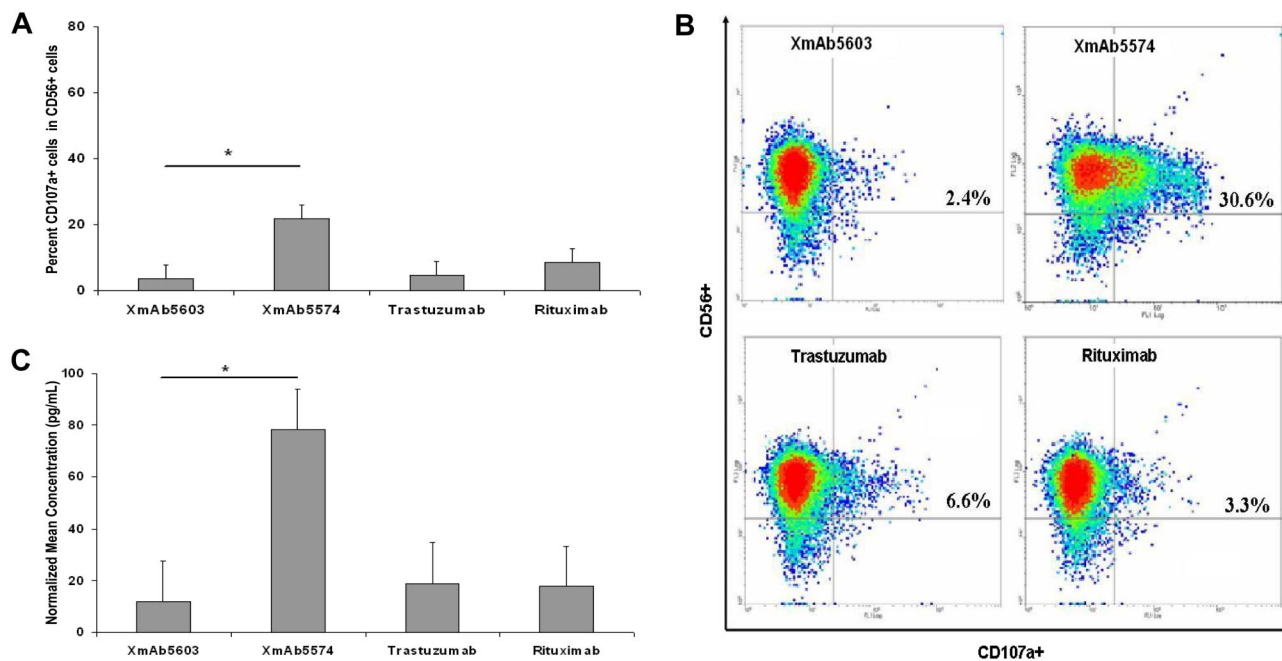


**Figure 4. XmaB5574 functionally activates NK cells.** (A) XmaB5574-mediated NK-cell activation was determined by characterization of surface expression of CD107a by FACS analysis on freshly isolated NK cells after 4-hour stimulation by 20  $\mu$ g/mL of respective antibody coated on a 96-well flat-bottom plate. XmaB5574 was significantly more effective in up-regulation of surface expression of CD107a than was XmaB5603 (19.4% higher; 95% CI, 9.6%-29.2%;  $P = .005$ ), trastuzumab (17.6% higher; 95% CI, 7.8%-27.4%;  $P = .006$ ), or rituximab (12.8% higher; 95% CI, 0.2%-25.3%;  $P = .04$ ;  $n = 5$ ). (B) Representative FACS density plots showing expression of CD107a in CD56<sup>+</sup> NK cells. Individual percentages of double-positive cells are shown in inserts. (C) NK-cell stimulation by fixed XmaB5574 resulted in a higher production of IFN- $\gamma$  in cell-free culture supernatant that was harvested after 4 hours and analyzed for levels of IFN- $\gamma$  by an enzyme-linked immunosorbent assay, compared with XmaB5603 (6.4 times higher; 95% CI, 2.13-19.19;  $P = .007$ ) or trastuzumab (4.68 times higher; 95% CI, 0.24-2.20;  $P = .008$ ) or rituximab (5.95 times higher; 95% CI, 2.3-15.41;  $P = .004$ ;  $n = 4$ ). Error bars represent SEMs.

binding by XmaB5574, no significant cytotoxicity was observed compared with the parent antibody or rituximab. This finding diminishes concern that XmaB5574 will be directly cytotoxic toward NK cells in vivo.

#### XmaB5574-mediated NK-cell ADCC against CLL cells can be enhanced further by lenalidomide

Recruitment of innate effector elements by therapeutic antibodies can occur through both engineering Fc-receptor binding, as with XmaB5574, but also by adding therapeutic agents to NK cells that enhance their cytotoxic potential. We have recently demonstrated that lenalidomide increases NK-cell expression of CD16 (Fc $\gamma$ RIII),<sup>15</sup> the receptor with high-affinity binding to XmaB5574. We therefore hypothesized that lenalidomide treatment might enhance XmaB5574-mediated NK-cell activation and also ADCC (Figure 6). Consistent with this finding, lenalidomide significantly enhanced ADCC by XmaB5574 (20.6% increased compared with XmaB5603; 95% CI, 2.0%-39.2%;  $P = .03$ ;  $n = 21$ ; at E/T of 25:1). These results establish the feasibility of dual targeting of the innate immune system by agents such as lenalidomide that activate NK cells and also Fc-domain-engineered antibodies as an exciting concept for clinical trials in this disease.

## Discussion

Herein, we have described preclinical data with the novel Fc-domain-modified antibody XmaB5574 that supports it as a promising new therapy for the treatment of CLL. CD19 has been reported to have an antigen density of 17 705 ( $\pm$  8837) per cell compared with the commonly targeted CD20 antigen whose antigen density

was reported as 8018 ( $\pm$  9087) per cell.<sup>41</sup> Although XmaB5574 mediates modest direct cytotoxicity and ADCC similar to rituximab, the novel engineering of the Fc-domain promotes a significantly increased amount of NK cell-mediated ADCC against CLL cells compared with either the nonengineered humanized anti-CD19 XmaB5603 antibody or rituximab. The modest enhancement of ADCC may be due to the differential repertoire of Fc $\gamma$ R expression on macrophages<sup>42,43</sup> or to the relevance of this effector cell to antibodies bound to the CD19 antigen. A previous study has shown that anti-CD19 antibodies rely on NK cells<sup>40</sup> to mediate ADCC. These studies were extended further to show that XmaB5574 activates NK cells greater than other wild-type therapeutic antibodies as shown through enhanced IFN- $\gamma$  production, CD107a up-regulation, and intracellular Erk1/2 activation. NK cell-mediated killing of CLL cells was shown to occur through a granzyme B-dependent mechanism. Furthermore, enhanced NK cell-mediated killing of CLL cells is observed with innate immune-activating therapies for CLL such as lenalidomide. Collectively, these studies provide justification for moving XmaB5574 forward to clinical development in CLL as a monotherapy and in combination with other agents.

One question not addressed in previous preclinical studies with Fc-domain-engineered antibodies is the ability of agents that activate effector cells to further enhance NK cell-mediated cytotoxicity. Although several innate immune-enhancing therapies are available, we chose to focus on lenalidomide that has both demonstrable clinical activity in CLL and also enhances NK cell-mediated ADCC against primary CLL cells. The precise mechanism of lenalidomide-induced enhancement in NK cell-mediated ADCC is yet to be elucidated and may be either through granzyme B or Fas-Fas ligand-mediated pathways. In addition, previous

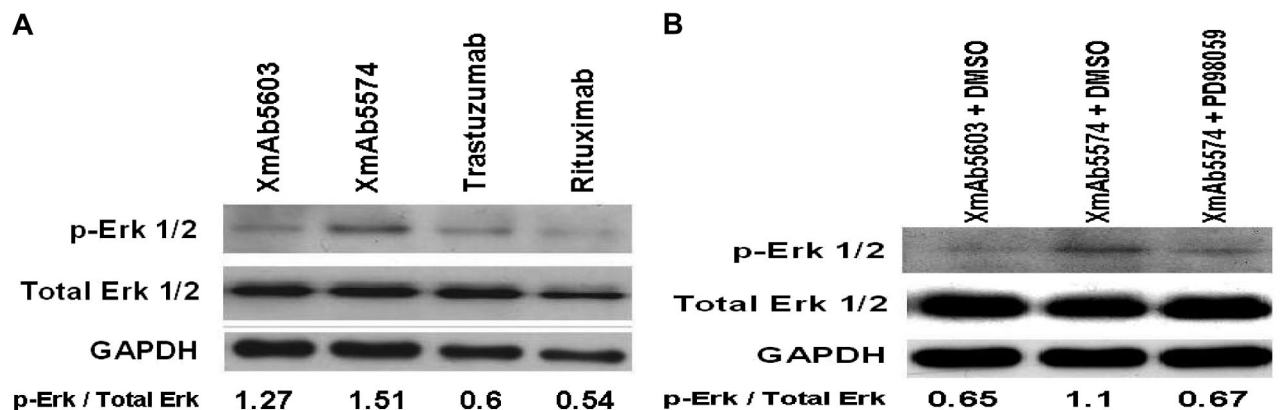


**Figure 5. XmAb5574 stimulation of NK cells results in up-regulation of Erk1/2 phosphorylation.** (A) Up-regulation of Erk1/2 phosphorylation in NK cells after stimulation by fixed XmAb5574 was detected by Western blot and compared with XmAb5603 and no antibody. Six-well flat-bottom plates were coated with 10 to 20  $\mu\text{g}/\text{mL}$  of respective antibody and then plated with freshly isolated NK cells at  $5 \times 10^6$  cells/well. NK cells were harvested after 10-minute incubation and immediately subjected to lysis and protein extraction. (B) Specific MEK kinase inhibitor PD98059 (100 $\mu\text{M}$ ) added to NK cells 30 minutes before their incubation with fixed XmAb5603 and XmAb5574 abrogates the enhancement of Erk1/2 phosphorylation by XmAb5574. Blots shown are representative of 3 individual experiments. Numbers denote densitometric ratios of p-Erk1/2 to total Erk1/2. (C) Ability of XmAb5574 to mediate ADCC against CLL cells through healthy donor NK cells was diminished but not significantly in the presence of media or PD98059 at 100 $\mu\text{M}$  (10.65% decrease with PD98059; 95% CI, 0.09-21.39; \* $P = .15$ ;  $n = 27$ ; compared with DMSO at E/T of 25:1). (D) Fixed XmAb5574 mediates minimal direct cytotoxicity against NK cells at 4 hours as shown by percentage of dead cells. Fixed antibody-mediated NK-cell cytotoxicity was determined by characterization of CD56 $^+$  and 7-AAD $^+$  cells by FACS analysis on freshly isolated NK cells after 4-hour stimulation by 20  $\mu\text{g}/\text{mL}$  of respective antibody coated on a 96-well flat-bottom plate. XmAb5574 did not mediate significantly higher NK-cell cytotoxicity than XmAb5603 (1% higher; 95% CI, -1.7% to 3.6%; \* $P = .4456$ ), trastuzumab (1% higher; 95% CI, -1.7% to 3.6%;  $P = .446$ ), or rituximab (0.8% higher; 95% CI, -1.8% to 3.5%;  $P = .518$ ;  $n = 4$ ). Percentage of dead cells was calculated as the number of 7-AAD $^+$  cells in the CD56 $^+$  cell population, and all values were normalized to media control. Error bars represent SEMs.

work performed by our group has shown that lenalidomide does not promote enhanced internalization of CD19 as shown by us to occur with CD20.<sup>15</sup> Herein, we have demonstrated that NK-cell activation and ADCC mediated by XmAb5574 can be further enhanced by pretreating NK cells with lenalidomide, which have previously been shown to enhance CD16 expression, and IFN- $\gamma$  secretion

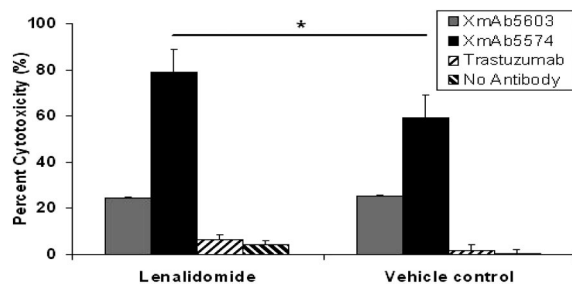


**Figure 6. Lenalidomide enhances XmAb5574-induced NK cell-mediated ADCC.** Ability of XmAb5574 to mediate ADCC against CLL cells through healthy donor NK cells was significantly enhanced by the pretreatment of NK cells with 0.5 $\mu\text{M}$  lenalidomide for 24 hours (20.6% higher ADCC with lenalidomide compared with vehicle control; 95% CI, 2.0%-39.2%; \* $P = .03$ ;  $n = 21$ ; at E/T of 25:1). Standard 4-hour  $^{51}\text{Cr}$ -release assay using patient CLL cells as target cells and healthy donor NK cells as effector cells was used. Error bars represent SEMs.

through phosphorylation of Erk1/2 proteins.<sup>44</sup> The addition of immunomodulating agents such as lenalidomide and the enhanced activation of NK cells that have been shown to be the primary mediators of ADCC in vitro,<sup>44,45</sup> by XmAb5574, is an exciting option for the management of patients with CLL and provides further rationale for the use of XmAb5574 in combination with lenalidomide. However, it is quite possible that other mechanisms of action, including stromal cell interactions, direct influence on tumor cells, and angiogenesis, may also be involved in lenalidomide mechanism of action in vivo in CLL cells.

Although our preclinical data with XmAb5574 show potential promise for clinical investigation in CLL, there are potential pitfalls to be considered as this therapeutic antibody moves forward to the clinic. XmAb5574 binds to CD19 but shows concentration- and time-dependent internalization similar to other CD19 and CD5 antibodies that have been described.<sup>46,47</sup> Although our studies in Figure 1C show continued expression of CD19 on the external portion of the CLL cells, it is possible that the internalization observed with this antibody could compromise its efficacy compared with clinically used antibodies such as alemtuzumab and rituximab that internalize less. In vivo studies with XmAb5574 in xenograft models suggest that it will maintain its efficacy.<sup>13,40</sup> Ultimately, it will require performance of a clinical trial of this



therapeutic in CLL to determine whether XmAb5574 has therapeutic efficacy in CLL.

In summary, we have demonstrated promising *ex vivo* activity of XmAb5574 in effectively activating NK cells over other available B cell–specific therapeutic antibodies used for the treatment of CLL. On the basis of the exciting preclinical data presented, further clinical development of XmAb5574 in CLL and other lymphoproliferative disorders is warranted.

## Acknowledgments

This work was supported by the D. Warren Brown Foundation, the Specialized Center of Research from the Leukemia & Lymphoma Society, the National Cancer Institute (P01 CA95426 and P01 CA81534), and the American Society of Clinical Oncology.

## Authorship

Contribution: F.T.A. designed the research, performed research, analyzed data, and wrote and reviewed the paper; R.L. designed the research, performed research, analyzed data, and reviewed the paper; R.T. performed the NK-cell signaling research, analyzed data, and reviewed the paper; J.P.B. performed the monocyte

ADCP research, analyzed data, and reviewed the paper; B.Y. and C.C. performed research, analyzed data, and reviewed the paper; D.M.B. designed the NK-cell research and reviewed the paper; J.M.R. performed early research, designed research, and reviewed the paper; X.M., A.L. analyzed data and reviewed the paper; J.J. provided essential CLL samples for analysis and reviewed the paper; J.F. provided essential CLL samples for analysis and reviewed the paper; D.J. and M.A.C. designed the research, analyzed data, and reviewed the paper; J.R.D. provided essential reagents, provided guidance on the research, and reviewed the paper; S.T. designed the monocyte ADCP research, analyzed data, and reviewed the paper; and N.M. and J.C.B. together originated the project, obtained funding for the project, designed research, analyzed data, helped review the different versions of the drafted paper, and approved the final version for submission.

Conflict-of-interest disclosure: J.R.D. has declared a financial interest in and is employed by a company whose product was studied in the present work. The remaining authors declare no competing financial interests.

XmAb5574 and XmAb5603 are registered trademarks of Xenor Inc.

Correspondence: Natarajan Muthusamy, 455E, OSUCCC, 410 W 12th Ave, Columbus, OH 43210; e-mail: raj.muthusamy@osumc.edu; or John C. Byrd, 455B, OSUCCC, 410 W 12th Ave, Columbus, OH 43210; e-mail: john.byrd@osumc.edu.

## References

- Martin P, Leonard JP. Targeted therapies for non-Hodgkin lymphoma: rationally designed combinations. *Clin Lymphoma Myeloma*. 2007;7(suppl 5):S192-S198.
- Sato S, Steeber DA, Jansen PJ, Tedder TF. CD19 expression levels regulate B lymphocyte development: human CD19 restores normal function in mice lacking endogenous CD19. *J Immunol*. 1997;158(10):4662-4669.
- Fujimoto M, Poe JC, Hasegawa M, Tedder TF. CD19 regulates intrinsic B lymphocyte signal transduction and activation through a novel mechanism of processive amplification. *Immunol Res*. 2000;22(2-3):281-298.
- Krop I, Shaffer AL, Fearon DT, Schissel MS. The signaling activity of murine CD19 is regulated during cell development. *J Immunol*. 1996;157(1):48-56.
- Sato S, Miller AS, Howard MC, Tedder TF. Regulation of B lymphocyte development and activation by the CD19/CD21/CD81/Leu 13 complex requires the cytoplasmic domain of CD19. *J Immunol*. 1997;159(7):3278-3287.
- Carter RH, Doody GM, Bolen JB, Fearon DT. Membrane IgM-induced tyrosine phosphorylation of CD19 requires a CD19 domain that mediates association with components of the B cell antigen receptor complex. *J Immunol*. 1997;158(7):3062-3069.
- Engel P, Zhou LJ, Ord DC, Sato S, Koller B, Tedder TF. Abnormal B lymphocyte development, activation, and differentiation in mice that lack or overexpress the CD19 signal transduction molecule. *Immunity*. 1995;3(1):39-50.
- Rickert RC, Rajewsky K, Roes J. Impairment of T-cell-dependent B-cell responses and B-1 cell development in CD19-deficient mice. *Nature*. 1995;376(6538):352-355.
- Sato S, Steeber DA, Tedder TF. The CD19 signal transduction molecule is a response regulator of B-lymphocyte differentiation. *Proc Natl Acad Sci U S A*. 1995;92(25):11558-11562.
- Hekman A, Honselaar A, Vuist WM, et al. Initial experience with treatment of human B cell lymphoma with anti-CD19 monoclonal antibody. *Cancer Immunol Immunother*. 1991;32(6):364-372.
- Hooijberg E, van den Berk PC, Sein JJ, et al. Enhanced antitumor effects of CD20 over CD19 monoclonal antibodies in a nude mouse xenograft model. *Cancer Res*. 1995;55(4):840-846.
- Lazar GA, Dang W, Karki S, et al. Engineered antibody Fc variants with enhanced effector function. *Proc Natl Acad Sci U S A*. 2006;103(11):4005-4010.
- Horton HM, Bennett MJ, Pong E, et al. Potent *in vitro* and *in vivo* activity of an Fc-engineered anti-CD19 monoclonal antibody against lymphoma and leukemia. *Cancer Res*. 2008;68(19):8049-8057.
- Cheson BD, Bennett JM, Grever M, et al. National Cancer Institute-sponsored Working Group guidelines for chronic lymphocytic leukemia: revised guidelines for diagnosis and treatment. *Blood*. 1996;87(12):4990-4997.
- Lapalombella R, Yu B, Triantafyllou G, et al. Lenalidomide down-regulates the CD20 antigen and antagonizes direct and antibody-dependent cellular cytotoxicity of rituximab on primary chronic lymphocytic leukemia cells. *Blood*. 2008;112(13):5180-5189.
- Bernhagen J, Krohn R, Lue H, et al. MIF is a non-cognate ligand of CXC chemokine receptors in inflammatory and atherogenic cell recruitment. *Nat Med*. 2007;13(5):587-596.
- Kondadasula SV, Roda JM, Parihar R, et al. Colocalization of the IL-12 receptor and FcγmAb11a to natural killer cell lipid rafts leads to activation of ERK and enhanced production of interferon-γ. *Blood*. 2008;111(8):4173-4183.
- Gellert GC, Kitson RP, Goldfarb RH. Urokinase-type plasminogen activator receptor crosslinking in an NK cell line increases integrin surface expression by the MAP kinase/ERK 1/2 signaling pathway. *J Cell Biochem*. 2003;89(2):279-288.
- Byrd JC, Shinn C, Waselenko JK, et al. Flavopiridol induces apoptosis in chronic lymphocytic leukemia cells via activation of caspase-3 without evidence of bcl-2 modulation or dependence on functional p53. *Blood*. 1998;92(10):3804-3816.
- Ingle GS, Chan P, Elliott JM, et al. High CD21 expression inhibits internalization of anti-CD19 antibodies and cytotoxicity of an anti-CD19-drug conjugate. *Br J Haematol*. 2008;140(1):46-58.
- Gerber HP, Kung-Sutherland M, Stone I, et al. Potent antitumor activity of the anti-CD19 auristatin antibody drug conjugate hBU12-vcMMAE against rituximab-sensitive and -resistant lymphomas. *Blood*. 2009;113(18):4352-4361.
- Pedersen IM, Buhl AM, Klausen P, Geisler CH, Jurlander J. The chimeric anti-CD20 antibody rituximab induces apoptosis in B-cell chronic lymphocytic leukemia cells through a p38 mitogen activated protein-kinase-dependent mechanism. *Blood*. 2002;99(4):1314-1319.
- Stanglmaier M, Reis S, Hallek M. Rituximab and alemtuzumab induce a nonclassical, caspase-independent apoptotic pathway in B-lymphoid cell lines and in chronic lymphocytic leukemia cells. *Ann Hematol*. 2004;83(10):634-645.
- Mone AP, Cheney C, Banks AL, et al. Alemtuzumab induces caspase-independent cell death in human chronic lymphocytic leukemia cells through a lipid raft-dependent mechanism. *Leukemia*. 2006;20(2):272-279.
- Smolewski P, Szmigielska-Kaplon A, Cebula B, et al. Proapoptotic activity of alemtuzumab alone and in combination with rituximab or purine nucleoside analogues in chronic lymphocytic leukemia cells. *Leuk Lymphoma*. 2005;46(1):87-100.
- Byrd JC, O'Brien S, Flinn IW, et al. Phase 1 study of lumiliximab with detailed pharmacokinetic and pharmacodynamic measurements in patients with relapsed or refractory chronic lymphocytic leukemia. *Clin Cancer Res*. 2007;13(15 pt 1):4448-4455.
- Alinari L, Hertlein E, Goldenberg DM, et al. Combination anti-CD74 (Milatuzumab) and CD20 (Rituximab) monoclonal antibody therapy has *in vitro* and *in vivo* activity in mantle cell lymphoma [abstract]. *Blood*. 2008;112(11):Abstract 886.
- Mone AP, Huang P, Pelicano H, et al. Hu1D10 induces apoptosis concurrent with activation of the AKT survival pathway in human chronic lymphocytic leukemia cells. *Blood*. 2004;103(5):1846-1854.

29. Hillmen P, Skotnicki AB, Robak T, et al. Alemtuzumab compared with chlorambucil as first-line therapy for chronic lymphocytic leukemia. *J Clin Oncol*. 2007;25(35):5616-5623.
30. Clarkson SB, Ory PA. CD16. Developmentally regulated IgG Fc receptors on cultured human monocytes. *J Exp Med*. 1988;167(2):408-420.
31. Anderson CL, Shen L, Eicher DM, Wewers MD, Gill JK. Phagocytosis mediated by three distinct Fc gamma receptor classes on human leukocytes. *J Exp Med*. 1990;171(4):1333-1345.
32. Vivier E, Tomasello E, Baratin M, Walzer T, Ugolini S. Functions of natural killer cells. *Nat Immunol*. 2008;9(5):503-510.
33. Penack O, Gentilini C, Fischer L, et al. CD56dimCD16neg cells are responsible for natural cytotoxicity against tumor targets. *Leukemia*. 2005;19(5):835-840.
34. Schoenborn JR, Wilson CB. Regulation of interferon-gamma during innate and adaptive immune responses. *Adv Immunol*. 2007;96:41-101.
35. Kim HY, Kim S, Chung DH. Fc gamma RIII engagement provides activating signals to NKT cells in antibody-induced joint inflammation. *J Clin Invest*. 2006;116(9):2484-2492.
36. Parihar R, Dierksheide J, Hu Y, Carson WE. IL-12 enhances the natural killer cell cytokine response to Ab-coated tumor cells. *J Clin Invest*. 2002;110(7):983-992.
37. Trotta R, Kanakaraj P, Perussia B. Fc gamma R-dependent mitogen-activated protein kinase activation in leukocytes: a common signal transduction event necessary for expression of TNF-alpha and early activation genes. *J Exp Med*. 1996;184(3):1027-1035.
38. Milella M, Gismondi A, Roncaioli P, et al. CD16 cross-linking induces both secretory and extracellular signal-regulated kinase (ERK)-dependent cytosolic phospholipase A2 (PLA2) activity in human natural killer cells: involvement of ERK, but not PLA2, in CD16-triggered granule exocytosis. *J Immunol*. 1997;158(7):3148-3154.
39. Trotta R, Puorro KA, Paroli M, et al. Dependence of both spontaneous and antibody-dependent, granule exocytosis-mediated NK cell cytotoxicity on extracellular signal-regulated kinases. *J Immunol*. 1998;161(12):6648-6656.
40. Zalevsky J, Leung IW, Karki S, et al. The impact of Fc engineering on an anti-CD19 antibody: increased Fc gamma receptor affinity enhances B-cell clearing in nonhuman primates. *Blood*. 2009;113(16):3735-3743.
41. D'Arena G, Dell'Olivo M, Musto P, et al. Morphologically typical and atypical B-cell chronic lymphocytic leukemias display a different pattern of surface antigenic density. *Leuk Lymphoma*. 2001;42(4):649-654.
42. Indik ZK, Park JG, Hunter S, Schreiber AD. The molecular dissection of Fc gamma receptor mediated phagocytosis. *Blood*. 1995;86(12):4389-4399.
43. Siberil S, Dutertre CA, Fridman WH, Teillaud JL. Fc gamma R: The key to optimize therapeutic antibodies? *Crit Rev Oncol Hematol*. 2007;62(1):26-33.
44. Wu L, Adams M, Carter T, et al. Lenalidomide enhances natural killer cell and monocyte-mediated antibody-dependent cellular cytotoxicity of rituximab-treated CD20+ tumor cells. *Clin Cancer Res*. 2008;14(14):4650-4657.
45. Zhao X, Lapalombella R, Joshi T, et al. Targeting CD37-positive lymphoid malignancies with a novel engineered small modular immunopharmaceutical. *Blood*. 2007;110(7):2569-2577.
46. Shawler DL, Johnson DE, McCallister TJ, Bartholomew RM, Dillman RO. Mechanisms of human CD5 modulation and capping induced by murine monoclonal antibody T101. *Clin Immunol Immunopathol*. 1988;47(2):219-229.
47. Press OW, Howell-Clark J, Anderson S, Bernstein I. Retention of B-cell-specific monoclonal antibodies by human lymphoma cells. *Blood*. 1994;83(5):1390-1397.